

Original Research



Association of Quantitative Flow Ratio with Lesion Severity and Its Ability to Discriminate Myocardial Ischemia

Neng Dai , MD^{1,*}, Doyeon Hwang , MD^{2,*}, Joo Myung Lee , MD, MPH, PhD³, Jinlong Zhang , MD², Yaliang Tong , MD⁴, Ki-Hyun Jeon , MD⁵, Jin Chul Paeng , MD, PhD⁶, Gi Jeong Cheon , MD, PhD⁶, Bon-Kwon Koo , MD, PhD^{2,7}, and Junbo Ge , MD¹

OPEN ACCESS

Received: Aug 26, 2020
Revised: Oct 9, 2020
Accepted: Nov 3, 2020

Correspondence to

Bon-Kwon Koo, MD, PhD

Department of Internal Medicine and Cardiovascular Center, Seoul National University Hospital, 101, Daehak-ro, Jongno-gu, Seoul 03080, Korea.
E-mail: bkkoo@snu.ac.kr

*Neng Dai and Doyeon Hwang contributed equally to this work.

Copyright © 2021. The Korean Society of Cardiology

This is an Open Access article distributed under the terms of the Creative Commons Attribution Non-Commercial License (<https://creativecommons.org/licenses/by-nc/4.0>) which permits unrestricted noncommercial use, distribution, and reproduction in any medium, provided the original work is properly cited.

ORCID iDs

Neng Dai
<https://orcid.org/0000-0003-3620-0699>
Doyeon Hwang
<https://orcid.org/0000-0002-0215-5319>
Joo Myung Lee
<https://orcid.org/0000-0002-2178-4014>
Jinlong Zhang
<https://orcid.org/0000-0003-4326-5087>
Yaliang Tong
<https://orcid.org/0000-0002-5646-3974>
Ki-Hyun Jeon
<https://orcid.org/0000-0002-6277-7697>
Jin Chul Paeng
<https://orcid.org/0000-0002-7464-9342>

¹Department of Cardiology, Zhongshan Hospital, Fudan University, Shanghai Institute of Cardiovascular Diseases, Shanghai, China

²Department of Internal Medicine and Cardiovascular Center, Seoul National University Hospital, Seoul, Korea

³Division of Cardiology, Department of Internal Medicine, Heart Vascular Stroke Institute, Samsung Medical Center, Sungkyunkwan University School of Medicine, Seoul, Korea

⁴Department of Cardiology, China-Japan Union Hospital of Jilin University, Jilin, China

⁵Department of Internal Medicine, Sejong General Hospital, Bucheon, Korea

⁶Department of Nuclear Medicine, Seoul National University Hospital, Seoul, Korea

⁷Institute on Aging, Seoul National University, Seoul, Korea

ABSTRACT

Background and Objectives: Quantitative flow ratio (QFR) is an angiography-based technique for functional assessment of coronary artery stenosis. This study investigated the response of QFR to different degree of stenosis severity and its ability to predict the positron emission tomography (PET)-defined myocardial ischemia.

Methods: From 109 patients with 185 vessels who underwent both ¹³N-ammonia PET and invasive physiological measurement, we compared QFR, fractional flow reserve (FFR) and instantaneous wave-free ratio (iFR) for the responses to the different degree of anatomical (percent diameter stenosis [%DS]) and hemodynamic (relative flow reserve [RFR], coronary flow reserve, hyperemic stenosis resistance, and stress myocardial flow) stenosis severity and diagnostic performance against PET-derived parameters.


Results: QFR, FFR, and iFR showed similar responses to both anatomic and hemodynamic stenosis severity. Regarding RFR, the diagnostic accuracy of QFR was lower than FFR (76.2% vs. 83.2%, p=0.021) and iFR (76.2% vs. 84.3%, p=0.031). For coronary flow capacity (CFC), QFR showed a lower accuracy than iFR (74.1% vs. 82%, p=0.031) and lower discriminant function than FFR (area under curve: 0.74 vs. 0.79, p=0.044). Discordance between QFR and FFR or iFR was shown in 14.6% of cases and was driven by the difference in %DS and heterogeneous distribution of PET-derived RFR and stress myocardial blood flow.

Conclusions: QFR demonstrated a similar response to different anatomic and hemodynamic stenosis severity as FFR or iFR. However, its diagnostic performance was inferior to FFR and iFR when PET-derived RFR and CFC were used as a reference.


Keywords: Coronary artery disease; Myocardial ischemia; Positron emission tomography

Gi Jeong Cheon 

<https://orcid.org/0000-0002-1360-5186>

Bon-Kwon Koo 

<https://orcid.org/0000-0002-8188-3348>

Junbo Ge 

<https://orcid.org/0000-0002-9360-7332>

Funding

Dr. Neng Dai acknowledges support by project 81600279 from the National Natural Science Foundation of China and project 2019M650075 from China Postdoctoral Science Foundation.

Conflict of Interest

Dr. Joo Myung Lee received a Research Grant from St. Jude Medical (Abbott Vascular) and Philips Volcano. Dr. Bon-Kwon Koo received an Institutional Research Grant from St. Jude Medical (Abbott Vascular) and Philips Volcano. All other authors declare that there is no conflict of interest relevant to the submitted work.

Author Contributions

Conceptualization: Dai N, Zhang J, Koo BK; Data curation: Hwang D, Lee JM, Tong Y, Jeon KH, Paeng JC, Cheon GJ, Koo BK; Formal analysis: Dai N, Hwang D, Koo BK; Investigation: Dai N, Hwang D; Methodology: Hwang D, Koo BK; Supervision: Lee JM, Zhang J, Paeng JC, Cheon GJ, Koo BK, Ge J; Validation: Hwang D, Lee JM, Zhang J, Ge J; Visualization: Hwang D; Writing - original draft: Dai N, Hwang D, Koo BK; Writing - review & editing: Dai N, Hwang D, Koo BK.

INTRODUCTION

Coronary physiologic assessment by fractional flow reserve (FFR) or instantaneous wave-free ratio (iFR) has become a standard method for identifying the ischemia causing coronary stenosis in the cardiac catheterization laboratory.¹ Despite the class IA recommendation of the measurement of FFR or iFR in the current guideline, real-world use is generally low and heterogeneous in different hospitals.^{2,3} Recently, the clinical application of computational fluid dynamics or mathematical assumptions has enabled the combination of data between coronary anatomy from imaging modalities and coronary physiology.^{4,5} Quantitative flow ratio (QFR) is one such modality which provides a 3-dimensional (3D) quantitative coronary angiography (QCA)-based FFR that can determine the hemodynamically significant lesion without pressure wire or hyperemia induction.⁵ Previous studies demonstrated its excellent diagnostic agreement with invasively-measured physiologic indices.⁵⁻¹¹ However, it should be noted that iFR and FFR are measured during resting and hyperemic status, respectively, while QFR uses a simulated hyperemic status of coronary circulation based on anatomical stenosis severity. In addition, no previous studies have investigated the association of QFR with positron emission tomography (PET)-derived hemodynamic indices in comparison with FFR and iFR.

In this regard, this study was conducted to investigate the association of QFR with different degrees of anatomic and hemodynamic lesion severity, and the diagnostic performance of QFR to predict PET-defined myocardial ischemia in comparison with FFR and iFR.

METHODS

Study population

The current study included the patients with available ¹³N-ammonia PET within 3 months of invasive physiologic assessment.¹² There was no intervention nor clinical event during the time between the PET scan and angiography/pressure measurement. Among a total of 144 patients, 15 patients with poor PET image quality, 2 patients without adequate coronary angiography data and 2 patients who underwent coronary bypass graft surgery were excluded. Patients with insufficient image quality for QFR analysis (calibration failure, ostial disease, insufficient projections, tortuous vessels, vessel overlap, or poor contrast filling) were also excluded and the specific reasons are presented in **Supplementary Figure 1**. Finally, 109 patients with 185 vessels were analyzed in this study. 3D QCA and analysis of QFR were retrospectively performed by an experienced analyst. The study protocol was approved by the ethics committee at Seoul National University Hospital (IRB No. H-1106-004-364) and was conducted in accordance with the Declaration of Helsinki.

¹³N-ammonia positron emission tomography protocol and quantification of myocardial blood flow and physiologic indices

All ¹³N-ammonia PET images were acquired during resting and hyperemic states by continuous intravenous infusion of adenosine (140 $\mu\text{g}\cdot\text{kg}^{-1}\cdot\text{min}^{-1}$) as previously described.¹³ A bolus of ¹³N-ammonium (370 MBq) was injected via a peripheral vein in both resting and hyperemic states, and list mode dynamic imaging was performed with a Siemens Biograph-40 PET/computed tomography scanner (Siemens Medical Solutions, Erlangen, Germany).¹⁴ A 2-compartment model was applied to quantify absolute myocardial blood flow (MBF, mL/min/g). The absolute MBF and physiological indices of a target segment were calculated from PET scan data.¹⁴ For image analysis and quantification of resting and stress

absolute MBF in milliliters per minute per gram of tissue image acquisition, Carimas software (Turku PET Center, Turku, Finland) was used. Parametric stress MBF polar maps were used to delineate defect areas in target myocardial territories and to obtain MBF values of target segments. PET-derived coronary flow reserve (CFR) was calculated as the ratio of hyperemic MBF to resting MBF in target segments.¹⁵⁾ Relative flow reserve (RFR) was calculated as the ratio of stress MBF in target myocardial segments to that of reference myocardial segments.¹⁶⁾ To compare the diagnostic performance of pressure-derived physiologic indices, CFR <2.0 and RFR ≤0.80 were used as reference ischemic standards. Coronary flow capacity (CFC) was defined as flow capacity combining maximum absolute MBF and CFR,¹⁷⁾ and ischemic cut-off values of 2.0 for CFR and 1.85 mL/min/g for stress MBF were used to define the presence of myocardial ischemia.¹⁸⁾ Hyperemic stenosis resistance (HSR) was calculated as mean stenosis pressure gradient divided by hyperemic MBF.

Offline computation of quantitative flow ratio

3D QCA and analysis of QFR were performed by an experienced analyst (AngioPlus; Pulse Medical Imaging Technology, Shanghai Co., Ltd., Shanghai, China) from an independent core laboratory at Zhongshan Hospital, Fudan University in a blinded fashion as previously described.⁵⁾ Briefly, end-diastolic frames of 2 optimal angiography projections, which were separated with angles of at least 25°, were selected and used for 3D model reconstruction. The 3D contour model of the segment of interest and its reference vessel were constructed in an automated manner and manual correction of contour was performed, if necessary. After acquisition of fixed QFR, estimated contrast coronary flow was calculated using thrombolysis in myocardial infarction (TIMI) frame-count adjustment, which indicated the frames where contrast entered and exited the segmented part of the vessel. With application of TIMI frame-count adjustment in the calculation method, the software automatically calculated the contrast QFR value. The ischemic cut-off value of contrast QFR ≤0.80 was used in the current study.

Invasive coronary angiography and measurement of physiological indices

Coronary angiography was performed with standard techniques. Angiographic views were obtained after the administration of intracoronary nitrate (100 or 200 µg). All angiograms were analyzed at a core laboratory (Seoul National University Hospital) by investigators blinded to other data. Two-dimensional (2D) QCA was performed using a validated software (CAAS II; Pie Medical System, Maastricht, Netherlands). Minimal lumen diameter, reference vessel size, and lesion length were measured, and percent diameter stenosis (%DS) was calculated.

All coronary physiological measurements were obtained after diagnostic angiography as previously described. Briefly, a 5F to 7F guide catheter was used to engage the coronary artery (**Supplementary Table 1**). A pressure-temperature sensor guide wire (Abbott Vascular, Santa Clara, CA, USA) was zeroed and equalized to aortic pressure, and then the pressure sensor was positioned at the distal segment of a target vessel. Intracoronary nitrate (100 or 200 µg) was administered before each physiological measurement. Continuous infusion of adenosine (140 µg·kg⁻¹·min⁻¹) was used to induce hyperemia. FFR was calculated as the mean distal coronary artery pressure/aortic pressure during hyperemia. All pressure data were collected and validated by investigators blinded to other data. iFR was calculated as the mean pressure distal to the stenosis divided by the mean aortic pressure during the diastolic wave-free period. Baseline tracing data of >5 heartbeats before adenosine infusion was extracted and then anonymized and coded as an ASCII text file. Those data were sent to the iFR core laboratory (Imperial College, London, UK), where iFR was calculated with fully automated algorithms acting over the wave-free period of a minimum of 5 beats.¹⁹⁾

Statistical analysis

Categorical variables were presented as numbers and relative frequencies. Continuous variables were presented as mean±standard deviation or median with interquartile range according to their distributions, which were checked by the Kolmogorov-Smirnov test. The Kruskal-Wallis test was used for comparison of continuous variables among the groups. Spearman correlation coefficients were calculated to evaluate the correlations among pressure physiologic indices, and polynomial regression was used to visualize the relationships between them. The Fisher r- to z-transformation was used to compare the difference between correlation coefficients.

The area under curve (AUC) was calculated from receiver operating characteristic (ROC) curve analysis and compared using with the DeLong method.²⁰ Diagnostic performance of pressure-derived physiological indices was presented with sensitivity, specificity, positive predictive value, negative predictive value, and diagnostic accuracy. They were compared using McNemar test (sensitivity, specificity, and accuracy) or weight generalized score statistic (positive predictive value and negative predictive value).

All probability values were 2-sided, and p value <0.05 was considered statistically significant. The statistical package R, version 3.4.3 (R Foundation for Statistical Computing, Vienna, Austria) was used for statistical analysis.

RESULTS

Patient and lesion characteristics

Baseline patient and lesion characteristics are presented in **Table 1**. The mean age was 64.3±9.0 years, and 95 patients (87.2%) were male. Mean % diameter stenosis from QCA, FFR, iFR, and QFR were 46.4±16.2%, 0.83±0.11, 0.92±0.12 and 0.84±0.13, respectively. The distributions of angiographic and physiologic indices are shown in **Supplementary Figure 2**. PET-derived RFR and CFR were 0.83±0.11 and 2.3±0.7, respectively.

Relationship between pressured-derived physiologic indices and stenosis severity

Figure 1 shows the correlations between pressured-derived physiological indices and anatomical stenosis severity. All 3 indices showed significant negative correlations with 2D %DS from QCA and 3D %DS from QFR analysis (all p values <0.001), while higher values of correlations were observed with 3D %DS than with 2D %DS. QFR showed higher correlations with %DS than FFR or iFR (all p values for comparison <0.05). All pressure-derived physiologic indices decreased along with the increase of hemodynamic stenosis severity such as RFR, CFR, stress MBE, and HSR (**Figure 2** and **Supplementary Table 2**). The degree of correlation was lower in QFR than that in FFR for RFR (0.655 vs. 0.786, p=0.008) and HSR (-0.797 vs. -0.950, p<0.001) (**Supplementary Figure 3** and **Supplementary Table 3**).

Diagnostic ability of quantitative flow ratio to predict positron emission tomography-defined myocardial ischemia

Table 2 and **Supplementary Figure 4** show the diagnostic performance of FFR, iFR and QFR against PET-derived RFR, CFR and CFC. With RFR as a reference standard, QFR showed lower sensitivity (58.5%) than FFR (70.8%, p value for comparison=0.011) and lower specificity (85.8%) than iFR (96.6%, p value for comparison=0.002), leading to

Table 1. Baseline patient and lesion characteristics

Characteristics	Values
Patient characteristics (n=109)	
Demographics	
Age (yr)	64.3±9.0
Male	95 (87.2)
Body mass index (kg/m ²)	24.4±2.3
Hypertension	81 (74.3)
Diabetes mellitus	39 (35.8)
Hypercholesterolemia	98 (89.9)
Current smoker	17 (15.6)
Family history of coronary artery disease	19 (17.4)
Prior myocardial infarction	13 (11.9)
Left ventricular ejection fraction (%)	60.6±6.2
Lesion characteristics (n=185)	
Lesion location	
LAD	91 (49.2)
LCX	54 (29.2)
RCA	40 (21.6)
QCA	
Reference diameter (mm)	2.8±0.5
2D diameter stenosis (%)	46.4±16.2
3D diameter stenosis (%)	41.6±12.8
Lesion length (mm)	12.2±8.9
Physiologic indices	
FFR	0.83±0.11
iFR	0.92±0.12
QFR	0.84±0.13
PET parameters	
CFR	2.3±0.7
RFR	0.83±0.11

Values are expressed as mean±standard deviation or number (%).

2D = 2-dimensional; 3D = 3-dimensional; CFR = coronary flow reserve; FFR = fractional flow reserve; LAD = left anterior descending artery; iFR = instantaneous wave-free ratio; LCX = left circumflex artery; PET = positron emission tomography; QCA = quantitative coronary angiography; QFR = quantitative flow ratio; RCA = right coronary artery; RFR = relative flow reserve.

the lower overall diagnostic accuracy of QFR (76.2%) than that of FFR (83.2%, p value for comparison=0.021) and iFR (84.3%, p value for comparison=0.031). With CFR as a reference, QFR showed lower specificity (80.7%) than iFR (89.6%, p value for comparison=0.013), but overall diagnostic accuracies of QFR, FFR and iFR were comparable. With CFC as a reference standard, QFR showed lower sensitivity (58.5%) than FFR (75.6%, p value for comparison=0.008) and lower specificity (78.5%) than iFR (87.1%, p value for comparison=0.008). The overall diagnostic accuracy of QFR (74.1%) was lower than that of iFR (82.0%, p value for comparison=0.031) against CFC.

The discriminant functions of QFR compared to FFR or iFR are shown in **Figure 3**. With RFR as a reference standard, the AUCs of FFR, iFR, and QFR were 0.899, 0.895 and 0.826, respectively. With CFC as a reference, the AUCs of FFR, iFR, and QFR were 0.788, 0.789 and 0.737, respectively. There was a significant difference only between FFR and QFR with both RFR and CFC as reference standards. With RFR as a reference, QFR showed a trend of lower discriminant function than iFR. There was no difference among AUCs of these 3 indices for CFR.

The diagnostic abilities of QFR in terms of diagnostic performance and discriminant function compared to FFR or iFR showed similar trends regardless of the target vessel location (**Supplementary Figures 5 and 6** and **Supplementary Tables 4 and 5**). In addition, QFR

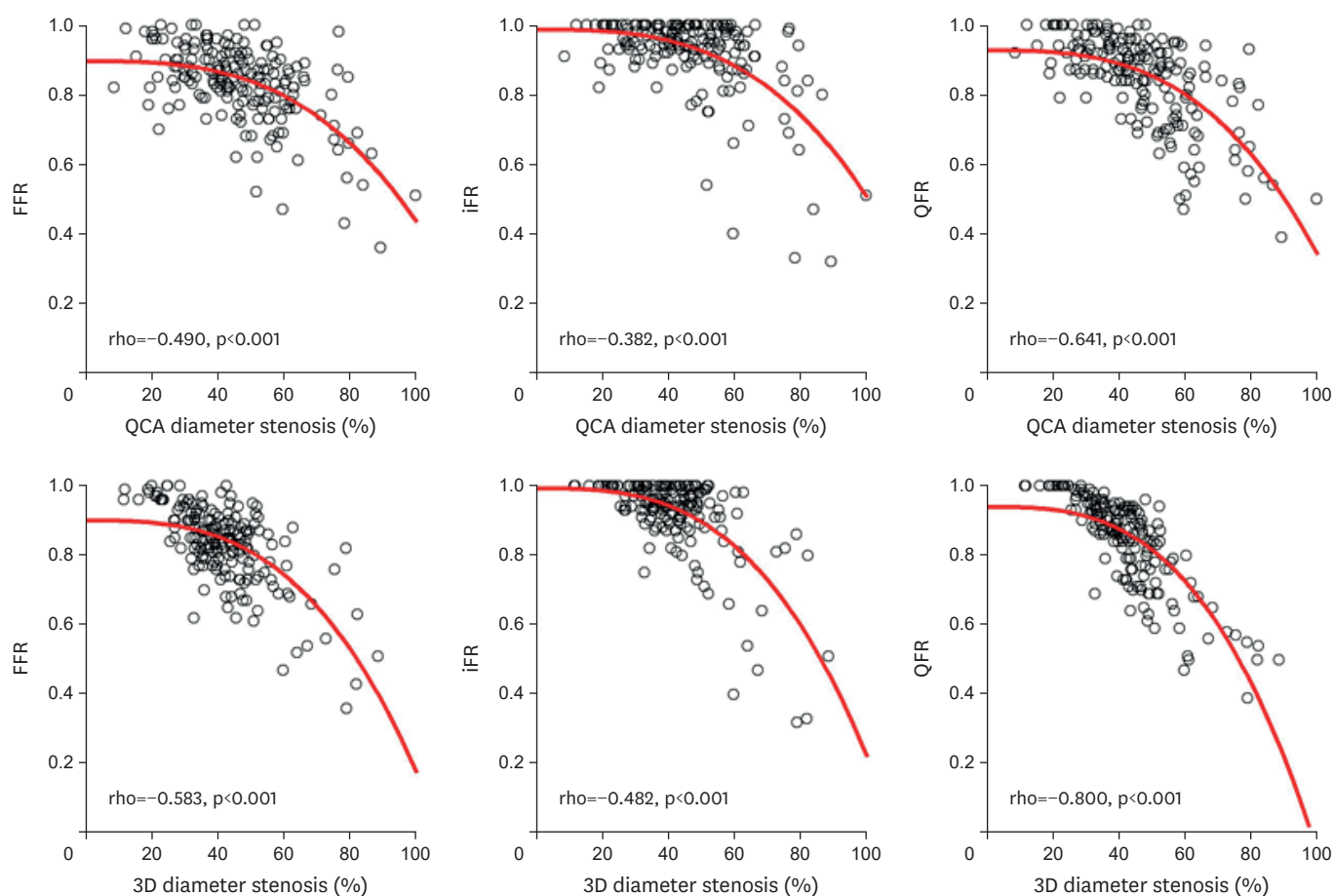


Figure 1. Correlations between angiographic severity and pressure-derived physiologic indices.

Correlations between 2D and 3D %DS and FFR, iFR and QFR are shown. There were significant correlations between 2D %DS and FFR, iFR and QFR, as well as 3D %DS and FFR, iFR and QFR. Redline was drawn using polynomial regression.

2D = 2-dimensional; 3D = 3-dimensional; FFR = fractional flow reserve; iFR = instantaneous wave-free ratio; %DS = percent diameter stenosis; QCA = quantitative coronary angiography; QFR = quantitative flow ratio.

showed high diagnostic performance to define myocardial ischemia in vessels which showed concordance results of pressure-derived and PET-derived indices (**Supplementary Table 6**).

Discordance between quantitative flow ratio and fractional flow reserve or instantaneous wave-free ratio

QFR showed significant correlations with FFR ($\rho = 0.820, p < 0.001$) and iFR ($\rho = 0.742, p < 0.001$) and 14.6% showed discordant results between QFR and FFR or iFR (**Supplementary Figure 7**). The anatomic and physiologic parameters in each accordant and discordant group are summarized in **Figure 4** and **Tables 3** and **4**. In both high FFR (A and B) and low FFR groups (C and D), there were differences in 2D and 3D %DS in high and low QFR groups (A vs. B, C vs. D). This finding was consistent with iFR and QFR comparisons. In contrast, PET-derived hemodynamic parameters showed different distribution patterns. For FFR-QFR comparison, there were no differences in RFR, CFR and hyperemic MBF between high and low QFR groups (A vs. B or C vs. D) in both high FFR and low FFR groups. For QFR and iFR comparison, the distribution of PET-derived hemodynamic parameters was similar except for stress MBF (**Figure 4**).

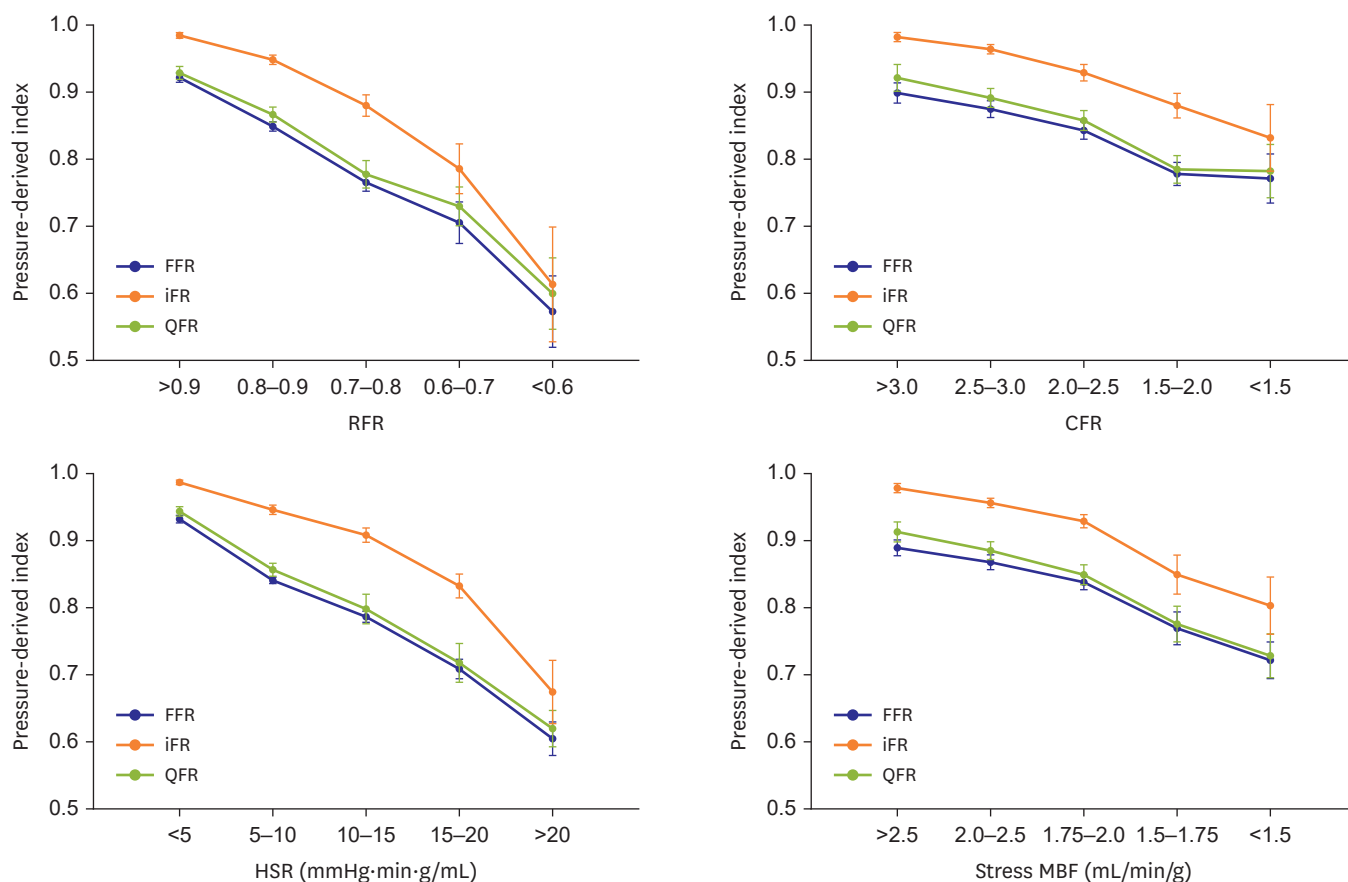


Figure 2. Pressure-derived physiologic indices according to hemodynamic severity groups.

This figure shows the values of FFR, iFR, and QFR, according to RFR, CFR, HSR and stress MBF. Solid circle and error bar mean the mean value and standard error, respectively.

FFR = fractional flow reserve; iFR = instantaneous wave-free ratio; RFR = relative flow reserve; CFR = coronary flow reserve; HSR = hyperemic stenosis resistance; MBF = myocardial blood flow; QFR = quantitative flow ratio.

Table 2. Comparison of diagnostic performance of FFR, iFR, and QFR against PET-derived indices

Diagnostic performance	FFR	iFR	QFR
RFR as a reference			
Sensitivity (%)	70.8 (59.7–81.8) [‡]	61.3 (49.2–73.4)	58.5 (46.5–70.4) [*]
Specificity (%)	90.0 (84.6–95.4) [†]	96.6 (93.2–99.9) ^{**}	85.8 (79.6–92.1) [†]
Positive predictive value (%)	79.3 (68.9–89.7)	90.5 (81.6–99.4) [‡]	69.1 (56.9–81.3) [†]
Negative predictive value (%)	85.0 (78.8–91.2) [‡]	82.4 (75.9–88.8)	79.2 (72.3–86.2) [*]
Diagnostic accuracy (%)	83.2 (83.1–83.4) [‡]	84.3 (84.1–84.4) [‡]	76.2 (76.0–76.4) ^{**†}
CFR as a reference			
Sensitivity (%)	53.0 (41.0–65.1)	47.6 (35.3–60.0)	48.5 (36.4–60.5)
Specificity (%)	80.7 (73.6–87.8) [†]	89.6 (84.0–95.2) ^{**}	80.7 (73.6–87.8) [†]
Positive predictive value (%)	60.3 (47.8–72.9) [†]	71.4 (57.8–85.1) ^{**}	58.2 (45.1–71.2) [†]
Negative predictive value (%)	75.6 (68.1–83.1)	75.7 (68.5–82.9)	73.8 (66.3–81.4)
Diagnostic accuracy (%)	70.8 (70.6–71.0)	74.7 (74.5–74.9)	69.2 (69.0–69.4)
CFC as a reference			
Sensitivity (%)	75.6 (62.5–88.8) ^{†‡}	63.2 (47.8–78.5) [*]	58.5 (43.5–73.6) [*]
Specificity (%)	81.2 (74.9–87.6) [†]	87.1 (81.6–92.7) ^{**}	78.5 (71.8–85.2) [†]
Positive predictive value (%)	53.4 (40.6–66.3) [‡]	57.1 (42.2–72.1) [‡]	43.6 (30.5–56.7) ^{**†}
Negative predictive value (%)	92.1 (87.4–96.8) [‡]	89.7 (84.6–94.8)	86.9 (81.1–92.7) [*]
Diagnostic accuracy (%)	80.0 (79.8–80.2)	82.0 (81.9–82.2) [‡]	74.1 (73.9–74.3) [†]

CFC = coronary flow capacity; CFR = coronary flow reserve; FFR = fractional flow reserve; iFR = instantaneous wave-free ratio; PET = positron emission tomography; QFR = quantitative flow ratio; RFR = relative flow reserve. *p<0.05 compared with FFR; †p<0.05 compared with iFR; ‡p<0.05 compared with QFR.

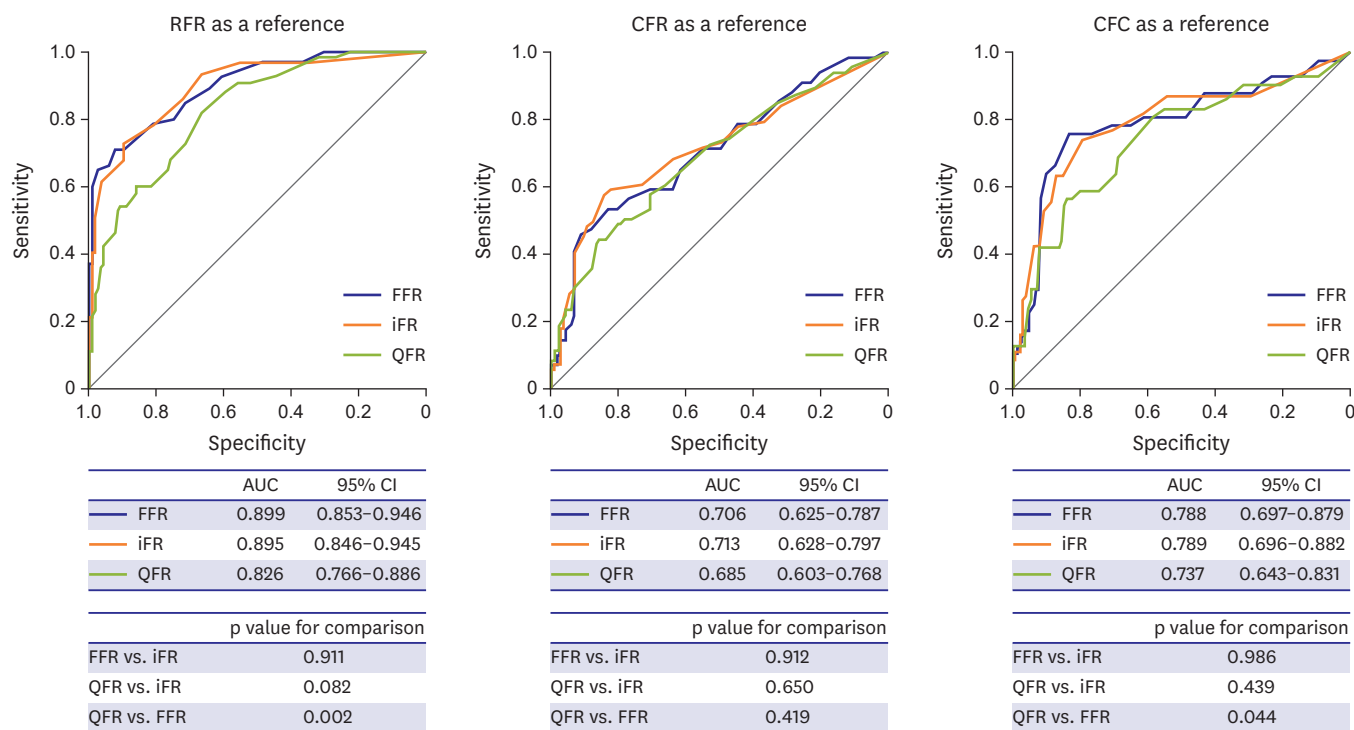
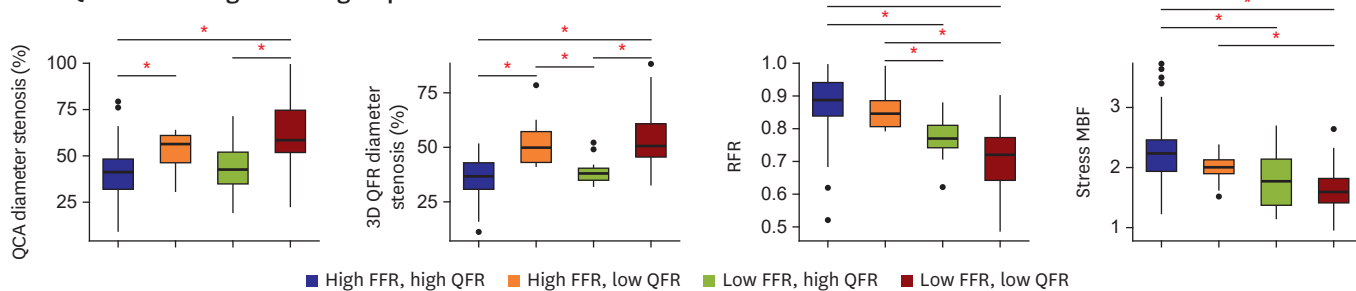


Figure 3. Discriminant functions of QFR, FFR and iFR against PET-derived indices.

Comparison of ROC curves of FFR, iFR, and QFR to predict RFR, CFR, and CFC are shown and AUCs are presented.

AUC = area under curve; CFC = coronary flow capacity; CFR = coronary flow reserve; CI = confidence interval; FFR = fractional flow reserve; iFR = instantaneous wave-free ratio; PET = positron emission tomography; QFR = quantitative flow ratio; RFR = relative flow reserve; ROC = receiver operating characteristic.

A 4 QFR and FFR agreement groups



B 4 QFR and iFR agreement groups

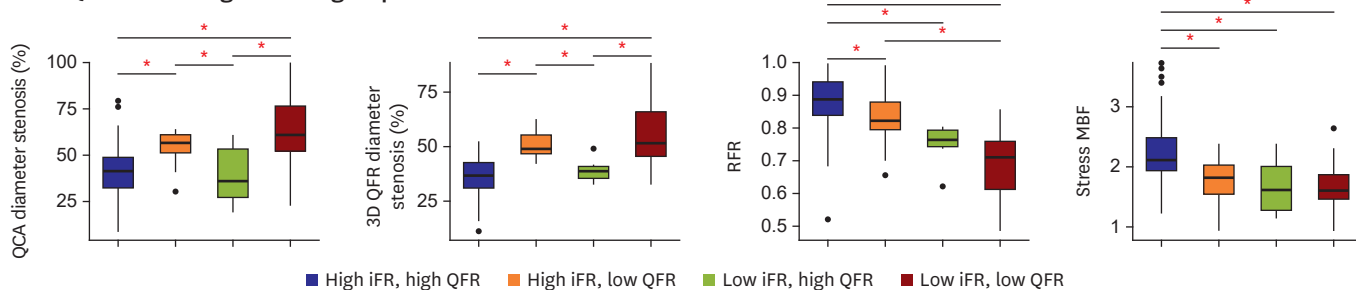


Figure 4. Anatomical and physiological severity according to QFR and FFR or iFR agreement.

The different distribution patterns of stenosis severity indices are shown in QFR and FFR agreement groups (A) and QFR and iFR agreement groups (B). The red star means a p value of <0.05. Each box ranges from upper quartile to lower quartile of the parameters and line inside the box indicates the location of the median value. The whiskers expand from the box to upper (upper quartile + 1.5×IQR) and lower (lower quartile - 1.5×IQR) extreme and outliers are plotted as individual dots.

FFR = fractional flow reserve; iFR = instantaneous wave-free ratio; IQR = interquartile range; QCA = quantitative coronary angiography; QFR = quantitative flow ratio.

Table 3. Physiologic and angiographic differences in patients among 4 FFR and QFR agreement groups

Parameters	Group A (n=115) (FFR >0.80 and QFR >0.80)	Group B (n=12) (FFR >0.80 and QFR ≤0.80)	Group C (n=15) (FFR ≤0.80 and QFR >0.80)	Group D (n=43) (FFR ≤0.80 and QFR ≤0.80)	p value
FFR	0.89 (0.85–0.94) ^{†§}	0.85 (0.83–0.87) ^{†§}	0.77 (0.77–0.79) ^{*†}	0.69 (0.64–0.75) ^{*†}	<0.001
QFR	0.93 (0.88–0.96) ^{†§}	0.75 (0.71–0.79) ^{*†}	0.86 (0.86–0.87) ^{*†§}	0.69 (0.59–0.74) ^{*†}	<0.001
Angiographic parameter					
Reference diameter (mm)	2.97 (2.63–3.29) [§]	2.44 (2.32–2.74)	2.74 (2.37–2.88)	2.59 (2.29–2.72) [*]	<0.001
2D diameter stenosis (%)	41.0 (31.5–48.0) ^{†§}	56.2 (46.7–60.8) [*]	42.6 (34.6–51.5) [§]	58.2 (51.9–74.6) ^{*†}	<0.001
3D diameter stenosis (%)	37.1 (31.0–43.2) ^{†§}	49.9 (43.3–57.2) ^{*†}	38.2 (35.3–40.3) ^{†§}	50.7 (45.8–60.8) ^{*†}	<0.001
Lesion length (mm)	8.1 (5.1–13.0) [§]	9.0 (6.1–22.5)	7.96 (6.8–12.0)	17.4 (7.8–28.6) [*]	<0.001
Parameters from PET					
PET derived RFR	0.89 (0.84–0.94) ^{†§}	0.85 (0.81–0.88) ^{†§}	0.77 (0.74–0.81) ^{*†}	0.72 (0.64–0.77) ^{*†}	<0.001
PET derived CFR	2.40 (2.05–2.73) [§]	2.05 (1.68–2.17)	2.10 (1.86–2.52)	1.89 (1.64–2.07) [*]	<0.001
Resting MBF (mL/min/g)	0.92 (0.83–1.02)	0.91 (0.86–1.25)	0.84 (0.78–0.96)	0.88 (0.76–1.03)	0.138
Stress MBF (mL/min/g)	2.09 (1.93–2.47) ^{†§}	2.00 (1.90–2.12) [§]	1.77 (1.37–2.14) [*]	1.60 (1.42–1.82) ^{*†}	<0.001

2D = 2-dimensional; 3D = 3-dimensional; CFR = coronary flow reserve; FFR = fractional flow reserve; PET = positron emission tomography; MBF = myocardial blood flow; QFR = quantitative flow ratio; RFR = relative flow reserve.

^{*}p<0.05 compared with group A; [†]p<0.05 compared with group B; [‡]p<0.05 compared with group C; [§]p<0.05 compared with group D.

Table 4. Physiologic and angiographic differences in patients among 4 iFR and QFR agreement groups

Parameters	Group A (n=118) (iFR >0.89 and QFR >0.80)	Group B (n=18) (iFR >0.89 and QFR ≤0.80)	Group C (n=8) (iFR ≤0.89 and QFR >0.80)	Group D (n=34) (iFR ≤0.89 and QFR ≤0.80)	p value
iFR	0.98 (0.94–1.00) ^{††§}	0.94 (0.92–0.97) ^{††§}	0.88 (0.86–0.89) ^{*†}	0.81 (0.70–0.87) ^{*†}	<0.001
QFR	0.93 (0.87–0.96) ^{†§}	0.74 (0.69–0.79) ^{*†}	0.87 (0.85–0.88) ^{†§}	0.67 (0.57–0.74) ^{*†}	<0.001
Angiographic parameter					
Reference diameter (mm)	2.97 (2.62–3.27) ^{†§}	2.60 (2.34–2.79) [*]	2.85 (2.79–2.87)	2.59 (2.28–2.71) [*]	<0.001
2D diameter stenosis (%)	41.0 (31.9–48.5) ^{†§}	56.3 (50.8–60.0) ^{*†}	35.6 (26.9–52.7) ^{†§}	60.5 (51.8–75.9) ^{*†}	<0.001
3D diameter stenosis (%)	36.7 (31.1–42.9) ^{†§}	48.9 (46.7–55.4) ^{*†}	39.0 (35.6–40.9) ^{†§}	51.4 (45.6–66.0) ^{*†}	<0.001
Lesion length (mm)	8.0 (5.1–13.0) ^{†§}	19.5 (8.9–24.2) ^{*†}	6.8 (5.7–10.8) ^{†§}	16.5 (7.7–25.7) ^{*†}	<0.001
Parameters from PET					
PET derived RFR	0.89 (0.83–0.94) ^{††§}	0.82 (0.79–0.88) ^{†§}	0.76 (0.74–0.79) [*]	0.71 (0.61–0.76) ^{*†}	<0.001
PET derived CFR	2.41 (2.06–2.78) ^{††§}	2.04 (1.71–2.22) [*]	1.90 (1.60–2.02) [*]	1.86 (1.64–2.03) [*]	<0.001
Resting MBF (mL/min/g)	0.89 (0.81–1.01)	0.86 (0.76–1.05)	0.96 (0.92–1.00)	0.89 (0.76–1.04)	0.910
Stress MBF (mL/min/g)	2.11 (1.93–2.48) ^{††§}	1.82 (1.54–2.03) [*]	1.61 (1.27–2.00) [*]	1.60 (1.46–1.86) [*]	<0.001

2D = 2-dimensional; 3D = 3-dimensional; CFR = coronary flow reserve; iFR = instantaneous wave-free ratio; PET = positron emission tomography; MBF = myocardial blood flow; QFR = quantitative flow ratio; RFR = relative flow reserve.

^{*}p<0.05 compared with group A; [†]p<0.05 compared with group B; [‡]p<0.05 compared with group C; [§]p<0.05 compared with group D.

DISCUSSION

The current study investigated QFR responses to different anatomic and hemodynamic stenosis severity as well as the diagnostic performance for flow impairment defined by PET in comparison with FFR and iFR. The main findings were as follows. First, QFR demonstrated a similar response as FFR and iFR to different anatomic and hemodynamic stenosis severity. Second, when compared with PET-derived RFR or CFC, the diagnostic performance of QFR was inferior to FFR or iFR. Third, discordance in stenosis classification between QFR and FFR or iFR was driven by the dependency of QFR on anatomical stenosis severity and individual differences in coronary physiologic conditions.

The clinical adoption of FFR or iFR still remains low,²⁾ possibly due to the need of additional instrumentation, high cost of pressure wires or operator reluctance.²¹⁾²²⁾ QFR is an index that can provide information on the functional significance of a lesion based on angiography-derived coronary anatomy and estimated coronary flow. This system does not require pressure wire interrogation or induction of hyperemia.⁵⁾ Despite the differences in the background of QFR with invasively measured FFR and iFR, previous studies demonstrated excellent correlation and diagnostic agreement of QFR for FFR⁵⁻¹⁰⁾ or iFR.¹⁰⁾¹¹⁾ In our current

study, QFR also demonstrated a strong relationship with FFR ($\rho=0.820$, $p<0.001$) or iFR ($\rho=0.742$, $p<0.001$). In addition, all QFR, FFR, and iFR showed significant correlation with anatomic and hemodynamic stenosis severity, indicating that QFR can be used as a physiologic index in the cardiac catheterization laboratory possibly like FFR and iFR. However, it should be noted that QFR cannot be measured in all cases, as the exclusion rate was 33.9% in our study. In addition, QFR is theoretically more dependent on anatomical stenosis severity than FFR and iFR and cannot fully reflect individual variations in coronary physiologic conditions. In our study, the correlations with QCA %DS and 3D %DS were higher with QFR than those with FFR or iFR.

In the current study, we employed PET-derived RFR, CFR and CFC as independent references to compare the diagnostic performance of QFR with FFR and iFR and showed that the diagnostic performance of these 3 indices were different according to the references. When using RFR as a reference standard, QFR demonstrated an inferior diagnostic accuracy and discriminant function compared with FFR. Diagnostic accuracy of iFR was also higher than QFR for RFR. For CFC, diagnostic accuracy of iFR was higher than QFR and discriminant function of FFR was higher than QFR. These results suggest that invasively measured physiologic assessment has better performance in defining ischemia-causing stenosis than QFR. It may be natural as QFR cannot reflect individual variations of coronary physiologic conditions, and the discordance between anatomical stenosis severity and functional significance of coronary stenosis.²³⁻²⁵⁾ It is interesting to note that the diagnostic performance of QFR was not different from that of FFR or iFR for PET-derived CFR. Moreover, the diagnostic performance of FFR, iFR, and QFR against CFR was lower than that against RFR. This may be because CFR is influenced by both macro- and microvascular disease status,¹²⁾¹⁴⁾²⁶⁾ while RFR is a more epicardial stenosis-specific parameter.¹⁶⁾

As QFR integrates both anatomical and physiological principles, its diagnostic performance is determined by the accuracy of both 3D coronary lumen reconstruction and assumed hemodynamic status. In our study population, the discordance between QFR and FFR or iFR was found in 14.6%. When these lesions were divided into 4 groups according to the cutoff values of QFR and FFR or iFR, 2D and 3D %DS were different between high and low QFR groups in both high FFR group and low FFR group. The high FFR but low QFR group demonstrated a numerically smaller reference diameter. One potential explanation might be that small coronary arteries make vessel demarcation more difficult, and even small variations in measurements may have a significant impact on the overall QCA quality and QFR calculation. Therefore, QFR results in small vessels may need to be interpreted with caution. This finding was similar in QFR and iFR relationship and suggests the dependency of QFR on anatomical stenosis severity. This is the common limitation of any anatomy-based physiologic assumption.²⁷⁾²⁸⁾ However, even this methodology is not based on full 3D curved geometry and cannot reflect individual variations of coronary physiologic characteristics.

As QFR is calculated from empirical hemodynamic assumptions, it may be natural to observe discordant results between QFR and invasively-measured physiologic parameters in some patients. Previous studies showed that resting and hyperemic flow conditions can influence the discordance between QFR and iFR or FFR.¹⁰⁾²⁵⁾ These authors reported that these discordances were mainly caused by the differences in patient-specific CFR or the presence of coronary microcirculatory dysfunction. In our study, the distribution patterns of anatomical and hemodynamics parameters were different among the 4 groups divided by QFR and FFR

or iFR. This result showed that both anatomical assessment and physiologic assumption of QFR determined the discordance between QFR and iFR or FFR.

There are several limitations in this study. First, this study was retrospectively investigated, and several patients were excluded due to insufficient angiography imaging quality for QFR and/or FFR or iFR pressure tracing artifacts. Second, the sample size of this study was relatively small, especially for the 4 group comparisons for the discrepancy between QFR and FFR or iFR, and further studies are warranted to confirm the results of our study findings. However, our study is the first one that compared the diagnostic performance of QFR with FFR and iFR using PET parameters as references. Third, ^{13}N -ammonia PET and invasive physiological measurements were not performed simultaneously. However, we included only patients with available ^{13}N -ammonia PET and FFR measurement within 3 months and there were no clinical events between the 2 tests. Fourth, we could not evaluate the prognostic implications of QFR-guided treatment. Fifth, this study used ^{13}N -ammonia as a PET tracer, and the absolute myocardial blood flow can be affected by the used tracer. However, the flow ratio, such as RFR or CFR, was reported to be relatively constant among different tracers.²⁹⁾ Finally, although PET demonstrated better diagnostic performance compared with other non-invasive modalities, high cost and limited availability are the limitations of PET in clinical practice.

In conclusion, QFR demonstrated a similar response to different anatomic and hemodynamic stenosis severities as FFR or iFR. However, its diagnostic performance was inferior to FFR and iFR when PET-derived RFR and CFC were used as a reference. The discordance between QFR and FFR or iFR was associated with the dependency of QFR on anatomical stenosis severity and individual variations in coronary physiologic conditions.

SUPPLEMENTARY MATERIALS

Supplementary Table 1

Information on the guide catheter size

[Click here to view](#)

Supplementary Table 2

Pressure-derived indices according to different ranges of hemodynamic severity

[Click here to view](#)

Supplementary Table 3

Correlations between pressure-derived physiologic indices and hemodynamic parameters

[Click here to view](#)

Supplementary Table 4

Comparison of diagnostic performance of FFR, iFR, and QFR against PET-derived indices in LAD

[Click here to view](#)

Supplementary Table 5

Comparison of diagnostic performance of FFR, iFR, and QFR against PET-derived indices in non-LAD

[Click here to view](#)

Supplementary Table 6

Diagnostic ability of QFR with concordance results of pressure-derived indices and PET-derived indices

[Click here to view](#)

Supplementary Figure 1

Study flow.

[Click here to view](#)

Supplementary Figure 2

Distributions of angiographic and physiologic indices.

[Click here to view](#)

Supplementary Figure 3

Associations between hemodynamic severity and pressure-derived physiologic indices.

[Click here to view](#)

Supplementary Figure 4

Diagnostic performance of FFR, iFR, and QFR against PET-derived indices.

[Click here to view](#)

Supplementary Figure 5

Discriminant functions of QFR, FFR, and iFR against PET-derived indices in LAD.

[Click here to view](#)

Supplementary Figure 6

Discriminant functions of QFR, FFR, and iFR against PET-derived indices in non-LAD.

[Click here to view](#)

Supplementary Figure 7

Discordance between QFR and FFR or iFR.

[Click here to view](#)

REFERENCES

1. Neumann FJ, Sousa-Uva M, Ahlsson A, et al. 2018 ESC/EACTS Guidelines on myocardial revascularization. *Eur Heart J* 2019;40:87-165.
[PUBMED](#) | [CROSSREF](#)
2. Dehmer GJ, Weaver D, Roe MT, et al. A contemporary view of diagnostic cardiac catheterization and percutaneous coronary intervention in the United States: a report from the CathPCI Registry of the National Cardiovascular Data Registry, 2010 through June 2011. *J Am Coll Cardiol* 2012;60:2017-31.
[PUBMED](#) | [CROSSREF](#)
3. Toth GG, Toth B, Johnson NP, et al. Revascularization decisions in patients with stable angina and intermediate lesions: results of the international survey on interventional strategy. *Circ Cardiovasc Interv* 2014;7:751-9.
[PUBMED](#) | [CROSSREF](#)
4. Tu S, Barbato E, Kőszegi Z, et al. Fractional flow reserve calculation from 3-dimensional quantitative coronary angiography and TIMI frame count: a fast computer model to quantify the functional significance of moderately obstructed coronary arteries. *JACC Cardiovasc Interv* 2014;7:768-77.
[PUBMED](#) | [CROSSREF](#)
5. Tu S, Westra J, Yang J, et al. Diagnostic accuracy of fast computational approaches to derive fractional flow reserve from diagnostic coronary angiography: the international multicenter FAVOR pilot study. *JACC Cardiovasc Interv* 2016;9:2024-35.
[PUBMED](#) | [CROSSREF](#)
6. Xu B, Tu S, Qiao S, et al. Diagnostic accuracy of angiography-based quantitative flow ratio measurements for online assessment of coronary stenosis. *J Am Coll Cardiol* 2017;70:3077-87.
[PUBMED](#) | [CROSSREF](#)
7. Collet C, Onuma Y, Sonck J, et al. Diagnostic performance of angiography-derived fractional flow reserve: a systematic review and Bayesian meta-analysis. *Eur Heart J* 2018;39:3314-21.
[PUBMED](#) | [CROSSREF](#)
8. Westra J, Andersen BK, Campo G, et al. Diagnostic performance of in-procedure angiography-derived quantitative flow reserve compared to pressure-derived fractional flow reserve: the FAVOR II Europe-Japan study. *J Am Heart Assoc* 2018;7:e009603.
[PUBMED](#) | [CROSSREF](#)
9. Westra J, Tu S, Winther S, et al. Evaluation of coronary artery stenosis by quantitative flow ratio during invasive coronary angiography: the WIFI II study (Wire-Free Functional Imaging II). *Circ Cardiovasc Imaging* 2018;11:e007107.
[PUBMED](#) | [CROSSREF](#)
10. Hwang D, Choi KH, Lee JM, et al. Diagnostic agreement of quantitative flow ratio with fractional flow reserve and instantaneous wave-free ratio. *J Am Heart Assoc* 2019;8:e011605.
[PUBMED](#) | [CROSSREF](#)
11. Emori H, Kubo T, Kameyama T, et al. Quantitative flow ratio and instantaneous wave-free ratio for the assessment of the functional severity of intermediate coronary artery stenosis. *Coron Artery Dis* 2018;29:611-7.
[PUBMED](#) | [CROSSREF](#)
12. Hwang D, Jeon KH, Lee JM, et al. Diagnostic performance of resting and hyperemic invasive physiological indices to define myocardial ischemia: validation with ¹³N-ammonia positron emission tomography. *JACC Cardiovasc Interv* 2017;10:751-60.
[PUBMED](#) | [CROSSREF](#)
13. Lee JM, Hwang D, Park J, et al. Exploring coronary circulatory response to stenosis and its association with invasive physiologic indexes using absolute myocardial blood flow and coronary pressure. *Circulation* 2017;136:1798-808.
[PUBMED](#) | [CROSSREF](#)
14. Lee JM, Kim CH, Koo BK, et al. Integrated myocardial perfusion imaging diagnostics improve detection of functionally significant coronary artery stenosis by ¹³N-ammonia positron emission tomography. *Circ Cardiovasc Imaging* 2016;9:e004768.
[PUBMED](#) | [CROSSREF](#)
15. Gould KL, Johnson NP, Bateman TM, et al. Anatomic versus physiologic assessment of coronary artery disease. Role of coronary flow reserve, fractional flow reserve, and positron emission tomography imaging in revascularization decision-making. *J Am Coll Cardiol* 2013;62:1639-53.
[PUBMED](#) | [CROSSREF](#)

16. Stuijffzand WJ, Uusitalo V, Kero T, et al. Relative flow reserve derived from quantitative perfusion imaging may not outperform stress myocardial blood flow for identification of hemodynamically significant coronary artery disease. *Circ Cardiovasc Imaging* 2015;8:e002400.
[PUBMED](#) | [CROSSREF](#)
17. Johnson NP, Gould KL. Integrating noninvasive absolute flow, coronary flow reserve, and ischemic thresholds into a comprehensive map of physiological severity. *JACC Cardiovasc Imaging* 2012;5:430-40.
[PUBMED](#) | [CROSSREF](#)
18. Hajjiri MM, Leavitt MB, Zheng H, Spooner AE, Fischman AJ, Gewirtz H. Comparison of positron emission tomography measurement of adenosine-stimulated absolute myocardial blood flow versus relative myocardial tracer content for physiological assessment of coronary artery stenosis severity and location. *JACC Cardiovasc Imaging* 2009;2:751-8.
[PUBMED](#) | [CROSSREF](#)
19. Sen S, Escaned J, Malik IS, et al. Development and validation of a new adenosine-independent index of stenosis severity from coronary wave-intensity analysis: results of the ADVISE (ADenosine Vasodilator Independent Stenosis Evaluation) study. *J Am Coll Cardiol* 2012;59:1392-402.
[PUBMED](#) | [CROSSREF](#)
20. DeLong ER, DeLong DM, Clarke-Pearson DL. Comparing the areas under two or more correlated receiver operating characteristic curves: a nonparametric approach. *Biometrics* 1988;44:837-45.
[PUBMED](#) | [CROSSREF](#)
21. Johnson NP, Koo BK. Coronary psychology: do you believe? *JACC Cardiovasc Interv* 2018;11:1492-4.
[PUBMED](#) | [CROSSREF](#)
22. Lee HS, Lee JM, Nam CW, et al. Consensus document for invasive coronary physiologic assessment in Asia-Pacific countries. *Cardiol J* 2019;26:215-25.
[PUBMED](#) | [CROSSREF](#)
23. Adjedj J, Xaplanteris P, Toth G, et al. Visual and quantitative assessment of coronary stenoses at angiography versus fractional flow reserve: the impact of risk factors. *Circ Cardiovasc Imaging* 2017;10:e006243.
[PUBMED](#) | [CROSSREF](#)
24. Toth G, Hamilos M, Pyxaras S, et al. Evolving concepts of angiogram: fractional flow reserve discordances in 4000 coronary stenoses. *Eur Heart J* 2014;35:2831-8.
[PUBMED](#) | [CROSSREF](#)
25. Mejía-Rentería H, Lee JM, Lauri F, et al. Influence of microcirculatory dysfunction on angiography-based functional assessment of coronary stenoses. *JACC Cardiovasc Interv* 2018;11:741-53.
[PUBMED](#) | [CROSSREF](#)
26. Johnson NP, Kirkeeide RL, Gould KL. Is discordance of coronary flow reserve and fractional flow reserve due to methodology or clinically relevant coronary pathophysiology? *JACC Cardiovasc Imaging* 2012;5:193-202.
[PUBMED](#) | [CROSSREF](#)
27. Johnson NP, Kirkeeide RL, Gould KL. Coronary anatomy to predict physiology: fundamental limits. *Circ Cardiovasc Imaging* 2013;6:817-32.
[PUBMED](#) | [CROSSREF](#)
28. Chu M, Dai N, Yang J, Westra J, Tu S. A systematic review of imaging anatomy in predicting functional significance of coronary stenoses determined by fractional flow reserve. *Int J Cardiovasc Imaging* 2017;33:975-90.
[PUBMED](#) | [CROSSREF](#)
29. Tahari AK, Lee A, Rajaram M, et al. Absolute myocardial flow quantification with ⁸²Rb PET/CT: comparison of different software packages and methods. *Eur J Nucl Med Mol Imaging* 2014;41:126-35.
[PUBMED](#) | [CROSSREF](#)